p-ISSN 2089 – 0133 e-ISSN 2477-6416
URL : https://jurnal.uns.ac.id/ijap/article/view/70436

Indonesian Journal of Applied Physics (IJAP) Vol. 13 No.2 page 207
DOI : https://doi.org/10.13057/ijap.v13i2.70436

EFFECT OF THE COMPOSITION OF TiO_2 ADDITIVES ON THE PHYSICAL AND MAGNETIC PROPERTIES, CRYSTAL STRUCTURE AND MICROSTRUCTURE OF $BaFe_{12}O_{19}$ MAGNETIC CERAMICS

Ramlan, Endah Puspita*

Physics department, Faculty of Mathematics and Natural Sciences, University of Sriwijaya, Palembang, Indonesia
*endahpuspita1908@gmail.com

Received 15-01-2023, Revised 17-02-2023, Accepted 15-07-2023
Available Online 15-07-2023, Published Regularly October 2023

ABSTRACT

A $BaFe_{12}O_{19}$ sample was prepared with variations in the addition of TiO_2 additives of 0%, 0.3%, 0.6% and 0.9% using the powder metallurgy method. The characterization carried out was density and porosity, X-Ray Diffraction (XRD), Scanning Electron Microscope (SEM), Vibrating Sample Magnetometer (VSM), and magnetic flux strength test. Based on the results of density and porosity, it shows that the $BaFe_{12}O_{19}$ sample with a variation of TiO_2 additive of 0%, 0.3%, 0.6%, and 0.9% has a density of 4.41 g/cm^3, 4.73 g/cm^3, 4.95 g/cm^3, and 4.72 g/cm^3, while the porosity was 5.45 g/cm^3, 3.79 g/cm^3, 2.15 g/cm^3, and 4.68 g/cm^3, respectively. From the XRD results, it shows that samples using additives and without TiO_2 additives produce $BaFe_{12}O_{19}$ phases, but there are still impurity phases that appear such as Fe_2O_3 (0% TiO_2), Ti_6O_{11} (0.3% and 0.9% TiO_2), and Ti_4O_7 (0.6 % TiO_2). From the SEM results, the morphology of the $BaFe_{12}O_{19}$ sample at 0.6% TiO_2 produced quite large grain particles, namely 0.5 – 1.5 μm. In VSM and magnetic flux, it shows that the $BaFe_{12}O_{19}$ sample is the highest hard magnetic at 0,6% variation with Ms, Mr, Hc respectively of 50.40 emu/gr, 23.20 emu/gr, 1.758 kOe and flux strength magnetic field of 272.65 Gauss.

Keywords: $BaFe_{12}O_{19}$; TiO_2; additives

Cite this as: Puspita, E., & Ramlan. 2023. Effect of The Composition of TiO_2 Additives on The Physical and Magnetic Properties, Crystal Structure and Microstructure of $BaFe_{12}O_{19}$ Magnetic Ceramics. *IJAP: Indonesian Journal of Applied Physics, 13*(2), 207-214. doi: https://doi.org/10.13057/ijap.v13i2.70436

INTRODUCTION

Barium Hexaferitte is a mixture of oxide compounds such as BaO and Fe_2O_3 which form the formula $BaFe_{12}O_{19}$ [1-2]. $BaFe_{12}O_{19}$ is often used in the manufacture of harvesting magnets [3]. This is because $BaFe_{12}O_{19}$ has the advantages of cheap raw material costs, high electrical resistivity of 108 Ω cm, high Curie temperature of 725°C, very stable and good corrosion resistance, and large magnetocrystalline anisotropy [4-5]. Permanent magnets are magnets that have permanent magnetic properties and are not easily lost [6]. Permanent magnets are widely used in various applications such as the electrical machinery and instrument industry, for example electric motors, electromagnetic transducers, and analog measuring devices with magnetic circuits [7–10]. The technique for making $BaFe_{12}O_{19}$ can be done physically and chemically. Physical techniques can be in the form of solid reaction methods [11], while chemical techniques can be in the form of sol-gel methods [12]. The magnetic properties, especially the coercivity of permanent magnets, depend on grain size where the coercive field of permanent magnets decreases with increasing grain size, while small grain sizes can increase the value of magnetic coercivity [13-15]. There are several additives that can affect grain size such as CuO, LaO, NaO, MnO, CaO, SiO_2, TiO_2 and others. In addition, additives can also be used to improve the physical, magnetic and microstructural properties of magnets [16-18].

Saragi et al (2012) made $BaFe_{12}O_{19}$ with the addition of additives, where this study used 3% CuO-TiO_2 as an additive and the sintering temperatures used were 1000°C, 1150°C and 1300°C. The resulting $BaFe_{12}O_{19}$ has good crystalline peak quality in the presence of additives and the impurity peaks decrease as the sintering temperature increases. The addition of additives in the manufacture of $BaFe_{12}O_{19}$ shows that additives can act as catalysts, so as to accelerate the growth rate in the formation of $BaFe_{12}O_{19}$ crystals without changing the structure and phase of $BaFe_{12}O_{19}$ crystals. In addition, grain growth on $BaFe_{12}O_{19}$ using additives produces smaller and more homogeneous grain sizes than without additives [19]. Furthermore, the effect of additives on magnetic properties has been explained by research conducted by Wardiyati et al (2020), where the additive used is Bi_2O_3 in the process of making $BaFe_{12}O_{19}$. The results show that the use of the Bi_2O_3 additive amount of 1.5% - 2% can produce a wide level of magnetic coercivity (hard magnetism) and high magnetic saturation (Ms). The high value of magnetic coercivity in $BaFe_{12}O_{19}$ is caused by low impurities. Additives can reduce the chance of growth of impurities during the process of forming $BaFe_{12}O_{19}$ using high sintering temperatures [20].

Research on the effect of adding additives such as TiO_2 to $BaFe_{12}O_{19}$ on grain size distribution, crystal structure and magnetic properties is currently still limited. Therefore, our research will be carried out in the manufacture of $BaFe_{12}O_{19}$ with the addition of TiO_2 additives using the powder metallurgy method.

METHOD

Preparation of $BaFe_{12}O_{19}$ Magnetic Ceramics

Barium Hexaferrite magnets are made using the powder metallurgy method. A total of 30 grams of $BaFe_{12}O_{19}$ powder was mixed with TiO_2 as an additive with variations in composition of 0%, 0.3%, 0.6% and 0.9% of the total $BaFe_{12}O_{19}$ powder, then milled for 3 hours. Dry the mixture in the oven at 105°C for 1 hour. The dried sample was added with 5% adhesive, namely Polyvinyl Alcohol (PVA), then the pellet sample was printed using a Hydraulic Press machine with a pressure of 8 tons and held for 1 minute, then the sample was sintered at 1000°C. The characterization used in this study was a physical property test (density and porosity), magnetic flux strength test, X-Ray Diffraction (XRD), Scanning Electron Microscope (SEM) and Vibrating Sample Magnetometer (VSM).

RESULT AND DISCUSSION

Density and Porosity

To determine the density and porosity of the sample can be seen in Figure 1. Figure 1 shows the density and porosity values of the $BaFe_{12}O_{19}$ samples depending on the use of TiO_2 additives. The variations of 0%, 0.3% and 0.6% TiO_2 showed an increase in the size of the density values of 4.41 g/cm3, 4.73 g/cm3 and 4.95 g/cm^3 respectively. The increase in density in the sample was due to the addition of the TiO_2 additive composition. However, at a variation of 0.9% TiO_2, the density decrease in the sample was 4.72 g/cm^3. This can be caused when the sample mixing process with PVA is not yet homogeneous. Mixing PVA with the sample functions as an interpenetrating network (IPN) which will fill the hydrogel cavities and the sample structure before the sintering process is carried out to make it tight and strong. In addition, for the sample porosity value is inversely proportional to the density. Porosity in the sample shows the level of cavity or pore volume contained in $BaFe_{12}O_{19}$ particles. Porosity in the sample decreased with increasing TiO_2 additives at variations of 0%, 0.3%, and 0.6%, namely 5.45 g/cm^3, 3.79 g/cm^3, 2.15 g/cm^3, respectively . However, at 0.9% TiO_2 variation there was an increase in porosity in the sample due to a decrease in the density value in the $BaFe_{12}O_{19}$ sample.

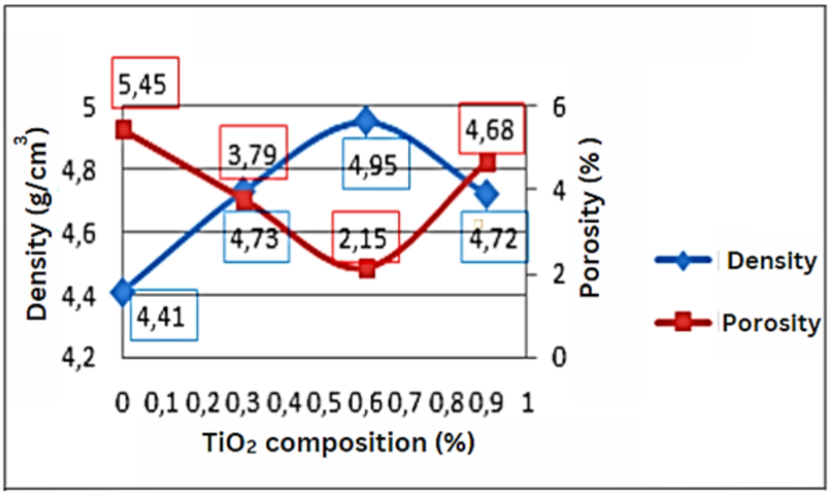

Figure 1. The relationship between density and porosity in the $BaFe_{12}O_{19}$ sample.

X-Ray Diffraction (XRD)

The crystal structure formed in the $BaFe_{12}O_{19}$ sample that has been analyzed by XRD can be seen in Figure 2. Figure 2 shows the diffraction peaks in the $BaFe_{12}O_{19}$ sample with variations in the addition of TiO_2 additives with variations of 0%, 0.3%, 0.6% and 0.9%. At 0% TiO_2 variation, two phases were formed, namely $BaFe_{12}O_{19}$ and Fe_2O_3. The $BaFe_{12}O_{19}$ phase formed is quite dominant compared to Fe_2O_3 and produces a crystal size of 0.171 nm. The highest peak is found in the Fe_2O_3 phase, namely at the angle 2θ of 35.50^o. Fe_2O_3 in the sample is an impurity phase, where this phase appears because the $BaFe_{12}O_{19}$ sample undergoes oxidation during the milling process. At a variation of 0.3% TiO_2, it shows that the phases formed are $BaFe_{12}O_{19}$ and Ti_6O_{11}. The highest peak is filled by the dominant phase with a fairly large intensity from the $BaFe_{12}O_{19}$ phase at an angle of 2θ of 35.74^o and the resulting crystal size is 17.505 nm. For the Ti_6O_{11} phase, it appears due to the presence of oxygen vacancies which allows defects to occur in the sample due to heat treatment or during the combustion process which is carried out at 1000^oC. If TiO_2 is treated with heat it will cause defects such as oxygen vacancies in the crystal lattice and the addition of Ti^{+6} interstitially or defects to form Ti_nO_{2n-1}. At a variation of 0.6% TiO_2, the phases formed are $BaFe_{12}O_{19}$ and Ti_4O_7. The $BaFe_{12}O_{19}$ phase produces a crystal size of 18.185 nm. The highest peak produced is located in the Ti_4O_7 phase at an angle of 2θ of 35.74^o. The phase difference formed by the effect of adding TiO_2 additives such as Ti_6O_{11} and Ti_4O_7 is the amount of composition and ions carried by Ti. For the 0.9% TiO_2 variation it also shows that the phases formed are $BaFe_{12}O_{19}$ and Ti_6O_{11} where the highest peak is located in the $BaFe_{12}O_{19}$ phase, namely with angle 2 which is $32,20^o$, and the $BaFe_{12}O_{19}$ crystal size obtained is 16.725 nm.

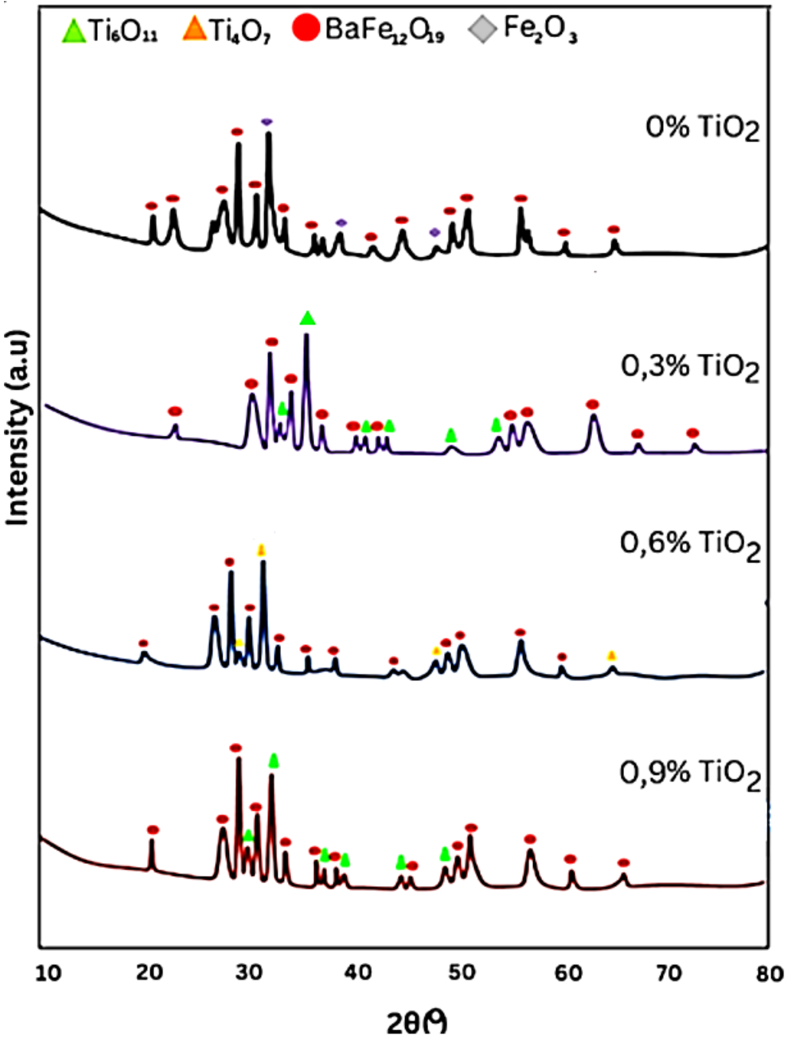

Figure 2. The peak of the diffraction pattern on the $BaFe_{12}O_{19}$ sample.

Vibrating Sample Magnetometer (VSM)

The magnetic properties of the $BaFe_{12}O_{19}$ sample can be seen through the hysteresis curve in Figure 3.

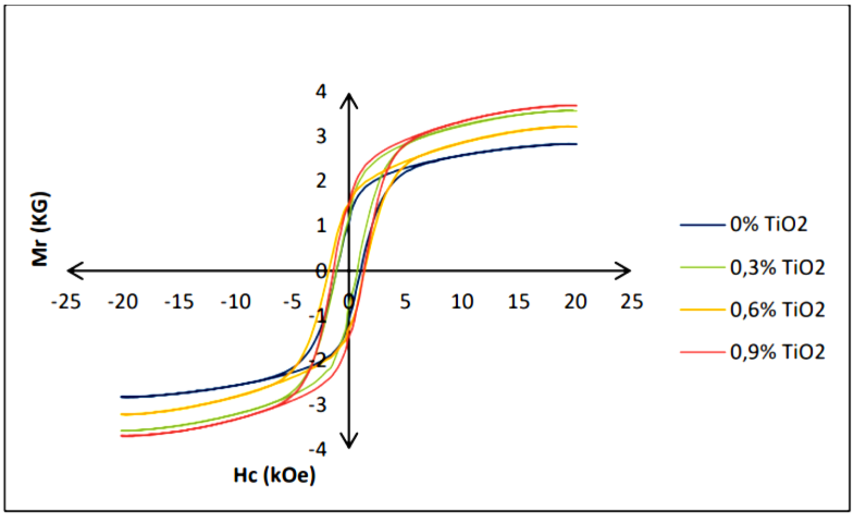

Figure 3. Hysteresis curve on the $BaFe_{12}O19$ sample.

Figure 3 shows the shape of the hysteresis curve in the $BaFe_{12}O_{19}$ sample, where the resulting curve shows a wide enough area where coercivity values exceeding 200 Oe are permanent magnets. At 0% TiO_2 variation, it shows that the $BaFe_{12}O_{19}$ sample produces saturation (Ms), remanence (Mr) and coercivity (Hc) values of 49.34 emu/gr, 18.59 emu/gr and 1.065 kOe, respectively. In this case the coercivity possessed by Barium Ferrite is greater than 200 Oe, so it can be concluded that the $BaFe_{12}O_{19}$ sample is classified as a permanent magnet [21]. At 0.3% TiO_2 variation, it shows that the $BaFe_{12}O_{19}$ sample experienced an increase in Ms, Mr, and Hc values, namely 58.91 emu/gr, 18.75 emu/gr 1.085 kOe, while at 0.6% TiO_2 it was 50.40 emu/gr, 23.20 emu/gr, 1.758 kOe. This is because with the addition of TiO_2 additives, Fe substitution by titanium ions occurs, where Ti^{+4} ions occupy positions $4f_1$ or $4f_2$ which are non-magnetic to replace some of Fe^{3+} which results in a reduction in the number of spin downs, thereby increasing the total magnetic moment in the sample. or improve its magnetic properties [22]. Fe^{3+} ion is a magnetic ion with a magnetic moment of 5µb and is located in three different positions in the crystal structure of Barium M-Hexaferite. The magnetic moment contribution for each position in one molecule of Barium M-Hexaferrite with positions 2a, 2b, and 12k on spin up and positions $4f_1$, $4f_2$ on spin down, where the total magnetic moment depends on the number of spin ups and spin downs in the material. The total magnetic moment in Barium M-Hexaferite ($BaFe_{12}O_{19}$) is 4 spin downs and 8 spin ups per crystal unit cell. Whereas in one crystal lattice $BaFe_{12}O_{19}$ has two crystal unit cells, which means it has 8 spin downs and 16 spin ups, resulting in a magnetic moment of 40 µb, each of which has a magnetic moment of Fe^{3+} ions of 5 µb [23]. At 0.9% TiO_2 variation, the magnetic coercivity value of the $BaFe_{12}O_{19}$ sample decreased. This decrease can be caused by a less homogeneous sample during the formation of $BaFe_{12}O_{19}$.

Magnetic Flux Strength

For the magnetic flux density of the BaFe12O19 sample using a gaussmeter and the results can be seen in Figure 4.

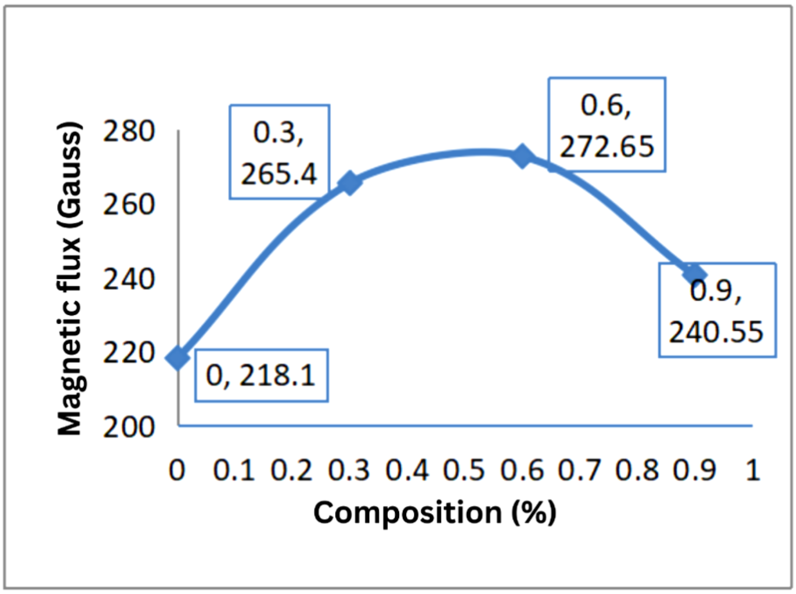

Figure 4. Magnetic flux strength on the $BaFe_{12}O_{19}$ sample.

From Figure 4 shows the magnetic flux strength contained in the $BaFe_{12}O_{19}$ sample. A density level of magnetic moments in a magnetic material is called magnetic flux, the magnetic flux density will increase depending on the number of magnetic moments contained in a material after being magnetized [24]. The strength of the magnetic flux increased from variations of 0%, 0.3% and 0.6% TiO_2, namely 218.0 Gauss, 265.40 Gauss and 272.65 Gauss, but decreased when the variation was 0.9% TiO_2 that is equal to 240.55 Gauss. This decrease may be caused by a defect in the resulting sample. In addition, the high value of the magnetic flux is caused by the high density value of a magnetic sample which can cause the rectifier magnetic dipole atomic moments to be closer and denser so that the magnetic flux value is greater.

Scanning Electron Microscope (SEM)

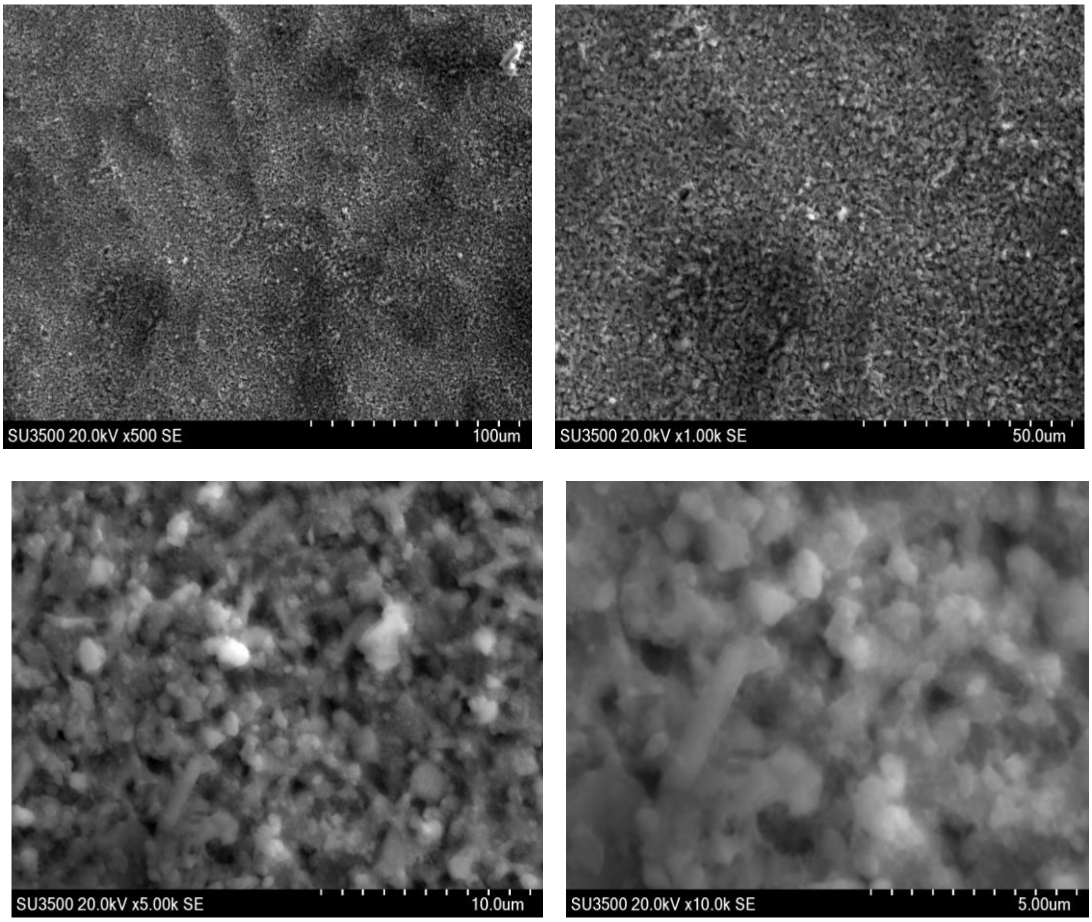

Figure 5. The morphology of the $BaFe_{12}O_{19}$ sample at 0.6% TiO_2 at magnifications of (a) 500 times, (b) 1.000 times, (c) 5.000 times and (d) 10.000 times.

Figure 5 shows the morphology of the $BaFe_{12}O_{19}$ sample at 0.6% TiO_2 variation, where the 0.6% TiO_2 variation is the best $BaFe_{12}O_{19}$ sample result compared to 0%, 0.3% and 0.9% variations. In the $BaFe_{12}O_{19}$ sample at a variation of 0.6% TiO_2, it shows grain particles that have a size of 0.5 – 1.5 μm and cavities between particles of 0.25 – 0.9 μm. For particles that have a size of more than 1 μm, it can be caused by the particles experiencing agglomeration. This is because if you use too much TiO_2 additive, a lot of TiO_2 grains will stick to $BaFe_{12}O_{19}$ particles so that they will produce large grains [17].

CONCLUSION

In this study, the $BaFe_{12}O_{19}$ sample was successfully synthesized using the powder metallurgy method. Based on XRD, samples using additives and without TiO_2 additives have succeeded in producing $BaFe_{12}O_{19}$ phases, but there are still impurity phases that appear such as Fe_2O_3 (0% TiO_2), Ti_6O_{11} (0.3% and 0.9% TiO_2), and Ti_4O_7 (0.6% TiO_2). For the density results in the sample, the density value increases with the addition of additives (0%, 0.3%, and 0.6% TiO_2), namely 4.41 g/cm^3, 4.73 g/cm^3, and 4.95 g/cm^3 while at a variation of 0.9% the sample decreased in density by 4.72 g/cm^3 due to the non-homogeneous sample. In addition, the porosity of the sample is inversely proportional to the density. Furthermore, based on the VSM and magnetic flux results, it was shown that the $BaFe_{12}O_{19}$ sample was the highest hard magnetic at 0.6% variation with a coercivity (Hc) of 1.758 kOe and a magnetic flux strength of 272.65 Gauss. For the SEM results, the morphology of the $BaFe_{12}O_{19}$ sample produced quite large particle grains, namely 0.5 – 1.5 μm, which was due to the sample undergoing agglomeration.

REFERENCES

1 Ramlan, D. Setiabudidaya, Suprapedi, A. A. Bama, & Muljadi. 2020. Study on the effect of CaO addition on micro structure and magnetic properties of BaFe12O19 made using powder metallurgy technique. *AIP Conf. Proc.*, 2221(110004), 1–5.

2 Rusianto, T., Wildan, M. W., Abraha, K., & Kusmono. 2015. Characterizations of ceramic magnets from iron sand. *Int. J. Technol.*, 6(6), 1017–1024.

3 Granados-Miralles, C., & Jenuš, P. 2021. On the potential of hard ferrite ceramics for permanent magnet technology-a review on sintering strategies. *J. Phys. D. Appl. Phys.*, 54(30), 1-14.

4 Ramlan, Muljadi, Sardjono, P., Setiabudidaya, D., & Gulo, F. 2019. Influence of addition Ba-Ferrite on the hardness, magnetic properties and corrosion resistance of hybrid bonded magnet NdFeB. *J. Phys. Conf. Ser.*, 1204(1), 1-5.

5 Salam, S. I., Sanjaya, E., & Muljadi, M. 2019. Pembuatan dan Karakterisasi Keramik Magnet BaFe12O19 dengan Variasi Waktu Milling dan Temperatur Sintering. *Al-Fiziya J. Mater. Sci. Geophys. Instrum. Theor. Phys.*, 2(1) 29–33.

6 Idayanti, N., Manaf, A., & Dedi. 2018. Magnet Nanokomposit sebagai Magnet Permanen Masa Depam. *Metalurgi*, 1(1), 1–18.

7 Slusarek, B., & Zakrzewski K. 2012. Magnetic properties of permanent magnets for magnetic sensors working in wide range of temperature, *Prz. Elektrotechniczny*, 88(7), 123–126.

8 Pangestuti, E. *et al.* 2017. Pengaruh Aditif Ferro Boron (FeB) terhadap Karakteristik Serbuk Hematit (α-Fe 2 O 3). *J. Teor. dan Apl. Fis.*, 5(2), 143–154.

9 Nugraha, P. R., Widanarto, W., Cahyanto, W. T., & Kuncoro, H. S. 2015. Pengaruh Aditif Baco3 Pada Kristalinitas Dan Suseptibilitas Barium Ferit Dengan Metoda Metalurgi Serbuk Isotropik. *Berk. Fis.*, 18(1), 43–50.

10 Bañuelos-Frías, A., Martínez-Guajardo, G., Alvarado-Perea, L., Canizalez-Dávalos, L., Ruiz, F., & Valero-Luna, C. 2019. Light absorption properties of mesoporous barium hexaferrite, BaFe12O19. *Mater. Lett.*, 252, 239–243.

11 Sari, A. Y., Safira, C. H., Setiadi, E. A., Simbolon, S., Kurniawan, C., & Sebayang, P. 2018. Efek Aditif FeMo dan Proses Kalsinasi pada Serbuk Magnetik BaFe12O19. *J. Sains Mater. Indones.*, 18(3). 95.

12 Kwak, J. Y., Lee, C. S., Kim, D., & Kim, Y. I. 2012. Characteristics of barium hexaferrite nanoparticles prepared by temperature-controlled chemical coprecipitation. *J. Korean Chem. Soc.*, 56(5), 609–616.

13 Humaidi, S., R. AS, T. R. S, S. D. S, & P. S. 2015. Magnetic Properties of Cu 2+ Subtituted BaFe12-xCuxO19 (x= 0.1,0.2,0.3,..., 4). *Indones. J. Appl. Phys.*, 5(1),71–78.

14 Anjum, S., Sehar, F., Mustafa, Z., & Awan, M. S. 2018. Enhancement of structural and magnetic properties of M-type hexaferrite permanent magnet based on synthesis temperature. *Appl. Phys. A Mater. Sci. Process.*, 124, 1-11.

15 Lee, J. S., Cha, J. M., Yoon, H. Y., Lee, J., & Kim, Y. K. 2015. Magnetic multi-granule nanoclusters : A model system that exhibits universal size effect of magnetic coercivity. *Nat. Publ. Gr.*, 1–7.

16 Töpfer, J., Schwarzer, S., Senz, S., & Hesse, D. 2005. Influence of SiO2 and CaO additions on the microstructure and magnetic properties of sintered Sr-hexaferrite. *J. Eur. Ceram. Soc.*, 25 (9), 1681–1688.

17 Haryadi, J., Muljadi., & Sebayang, P. 2007. Pengaruh Aditif SiO2 terhadap Sifat Fisis dan Sifat Magnet pada Pembuatan Magnet BaO.6Fe2O3. *J. Fis. Himpun. Fis. Indones.*, 7(1), 39–46.

18 Idayanti, N., Dedi, Kristiantoro, T., Mulyadi, D., Sudrajat, N., & Alam, G. F. N. 2018. Manufacture of barium hexaferrite (BaO3.98Fe2O3) from iron oxide waste of grinding process by using calcination process. *J. Phys. Conf. Ser.*, 985(1), 0–7.

19 Saragi, T., Syakir, N., Noelik, E., & Gustaman, D. 2012. Magnetic materials development of barium heksaferrite prepared from precipitation of yarosit and it’s characetrization. *Bionatura-Jurnal Ilmu-ilmu Hayati dan Fis.*, 14(2), 156–163.

20 Siswoyo, S. W., Winatapura, D. S., & Sukirman, E. 2017. Pengaruh Penambahan Aditif Bi2O3 Terhadap Karakteristik Barium Heksaferit Hasil Sintesis dengan Metode Sol-Gel. *J. Kim. dan Kemasan*, 39(2), 61.

21 Senida, Z. E., Ramli, Ratnawulan, & Hidayati. 2019. Pengaruh Variasi Komposisi MnFe2O4 Terhadap Sifat Magnetik Nanokomposit MnFe2O4/PANi yang Disintesis dengan Metoda Sol-Gel Spin Coating. *Pillar Phys.*, 12(2), 17–24.

22 Dairy, A. R. A., Al-Hmoud, L. A., & Khatatbeh, H. A. 2019. Magnetic and structural properties of Barium Hexaferrite nanoparticles doped with Titanium. *Symmetry (Basel).*, 11(6), 1–12.

23 Joni I., & Darminto, D. 2014. Penerapan Metode Sol-Gel dengan Variasi Temperatur dan Waktu Kalsinasi pada Sintesis Barium M-Heksaferit (BaFe12O19). *J. Fis. dan Apl.*, 10(1), 53-56.

24 Ritawanti, A., Sembiring, K., Muljadi, M., & Febrianto, E. Y. 2016. Pengaruh Ukuran Butir (grain size) pada pembuatan Bonded Magnet NdFeB. *J. Ikat. Alumni Fis.*, 2(1), 10-15.